Chinese Physics C

Measurement of $J/\psi \to \eta_c\gamma$ at KEDR[*]

V.V. Anashin[1] V.M. Aulchenko[1,2] E.M. Baldin[1,2] A.K. Barladyan[1] A.Yu. Barnyakov[1] M.Yu. Barnyakov[1]

S.E. Baru[1,2] I.V. Bedny[1] O.L. Beloborodova[1,2] A.E. Blinov[1] V.E. Blinov[1,3] A.V. Bobrov[1]

V.S. Bobrovnikov[1] A.V. Bogomyagkov[1,2] A.E. Bondar[1,2] A.R. Buzykaev[1] S.I. Eidelman[1,2]

Yu.M. Glukhovchenko[1] V.V. Gulevich[1] D.V. Gusev[1], S.E. Karnaev[1] G.V. Karpov[1] S.V. Karpov[1]

T.A. Kharlamova[1,2] V.A. Kiselev[1] S.A. Kononov[1,2] K.Yu. Kotov[1] E.A. Kravchenko[1,2]

V.F. Kulikov[1,2] G.Ya. Kurkin[1,3] E.A. Kuper[1,2] E.B. Levichev[1,3] D.A. Maksimov[1] V.M. Malyshev[1;1)]

A.L. Maslennikov[1] A.S. Medvedko[1,2] O.I. Meshkov[1,2] A.I. Milstein[1] S.I. Mishnev[1]

I.I. Morozov[1,2] N.Yu. Muchnoi[1,2] V.V. Neufeld[1] S.A. Nikitin[1] I.B. Nikolaev[1,2] I.N. Okunev[1]

A.P. Onuchin[1,3] S.B. Oreshkin[1] I.O. Orlov[1,2] A.A. Osipov[1] S.V. Peleganchuk[1] S.G. Pivovarov[1,3]

P.A. Piminov[1] V.V. Petrov[1] A.O. Poluektov[1] I.N. Popkov[1] G.E. Pospelov[1] V.G. Prisekin[1] A.A. Ruban[1]

V.K. Sandyrev[1] G.A. Savinov[1] A.G. Shamov[1] D.N. Shatilov[1] B.A. Shwartz[1,2] E.A. Simonov[1]

S.V. Sinyatkin[1] Yu.I. Skovpen[1,2] A.N. Skrinsky[1] V.V. Smaluk[1,2] A.V. Sokolov[1] A.M. Sukharev[1]

E.V. Starostina[1,2] A.A. Talyshev[1,2] V.A. Tayursky[1] V.I. Telnov[1,2] Yu.A. Tikhonov[1,2]

K.Yu. Todyshev[1,2] G.M. Tumaikin[1] Yu.V. Usov[1] A.I. Vorobiov[1] A.N. Yushkov[1] V.N. Zhilich[1]

V.V.Zhulanov[1,2] A.N. Zhuravlev[1,2]

1 (Budker Institute of Nuclear Physics, 11, Lavrentiev prospect, Novosibirsk, 630090, Russia)
2 (Novosibirsk State University, 2, Pirogova street, Novosibirsk, 630090, Russia)
3 (Novosibirsk State Technical University, 20, Karl Marx prospect, Novosibirsk, 630092, Russia)

Abstract We present a study of the inclusive photon spectra from 5.9 million J/ψ decays collected with the KEDR detector at the VEPP-4M e^+e^- collider. We measure the branching fraction of radiative decay $J/\psi \to \eta_c\gamma$, η_c width and mass. Our preliminary results are: $M(\eta_c) = 2979.4 \pm 1.5 \pm 1.9$ MeV/c^2, $\Gamma(\eta_c) = 27.8 \pm 5.1 \pm 3.3$ MeV, $\mathcal{B}(J/\psi \to \eta_c\gamma) = (2.34 \pm 0.15 \pm 0.40)\%$.

Key words η_c meson, full width, mass, radiative decay

PACS 13.20.Gd, 13.40.Hq, 14.40.Pq

1 Introduction

$J/\psi \to \eta_c\gamma$ decay is an M1 radiative transition with photon energy about 114 MeV, and a relatively large branching fraction about 2%. This is a transition between 1S states of charmonium, which rate can be easily calculated in potential models. However, for a long time a significant difference between theoretical predictions and experimental data was observed. Until the last year the PDG value of this branching was based on a single measurement[1] of Crystal Ball using an inclusive spectrum of photons in the J/ψ de-

cays with the result $\mathcal{B}(J/\psi \to \eta_c\gamma) = (1.27 \pm 0.36)\%$, approximately twice less than the theoretical predictions $3.05 \pm 0.07\%$[2], $2.4 \pm 0.3\%$[3], $2.1 \pm 0.4\%$[4]. For comparison, in E1 transitions of charmonium the corresponding difference is (20-30)% only[2], although the matrix element has more complex structure.

In 2009 CLEO published[5] a new measurement of this branching with the value $\mathcal{B}(J/\psi \to \eta_c\gamma) = (1.98 \pm 0.09 \pm 0.30)\%$, which is closer to theory. CLEO analysis used exclusive η_c decays and found that the line shape of this transition is asymmetric. A Breit-Wigner function (BW) alone provides a poor fit to

data. A Breit-Wigner modified by E_γ^3 (according to theoretical predictions for electromagnetic dipole transitions) improves the fit near a resonance, but gives a diverging tail at higher photon energies. To suppress this tail CLEO used an additional exponential factor.

2 Photon spectrum

The photon spectrum in $J/\psi \to \eta_c \gamma$ decay is given by the formula

$$\frac{dN_\gamma}{d\omega} = N_\psi \mathcal{B} \int_0^{M_\psi/2} d\omega' \frac{d\Gamma(\omega')}{d\omega'} \frac{\epsilon(\omega')g(\omega,\omega')}{\Gamma_{\eta_c\gamma}}, \qquad (1)$$

where $\mathcal{B}$ is the decay branching fraction, $g(\omega,\omega')$ is a calorimeter response function, $\epsilon(\omega)$ is a photon detection efficiency, $d\Gamma(\omega)/d\omega$ is a true photon spectrum, and $\Gamma_{\eta_c\gamma} = \int d\omega d\Gamma(\omega)/d\omega$ is the full decay width. The true photon spectrum can be written as [2]

$$\frac{d\Gamma(\omega)}{d\omega} = \frac{4}{3}\alpha \frac{e_c^2}{m_c^2}\omega^3 |M|^2 BW(\omega). \qquad (2)$$

Here $M = <\eta_c|j_0(\omega r/2)|J/\psi>$ is the matrix element of the transition, $j_0(x) = sin(x)/x$, e_c and m_c are c-quark charge and mass.

We see that if ω tends to zero, the matrix element tends to unity. CLEO used in their fit $|M|^2 = exp(-\omega^2/8\beta^2)$ with $\beta = 65$ MeV, but such a form of

matrix element squared is valid for harmonic oscillator wave functions only. In all other potentials $|M|^2$ dependence will be proportional to ω^{-n}.

Therefore we tried to fit the CLEO data using another line shape: at photon energy ω near resonance the decay probability $d\Gamma/d\omega$ is proportional to ω^3, but at higher energies the factor ω^3 is replaced with ω. We found that the function $d\Gamma/d\omega \sim \omega^3\omega_0^2/(\omega\omega_0+(\omega-\omega_0)^2))BW(\omega)$, where ω_0 is the most probable transition energy, is also suitable. In Fig. 1, our fit of CLEO data using such a function is shown.
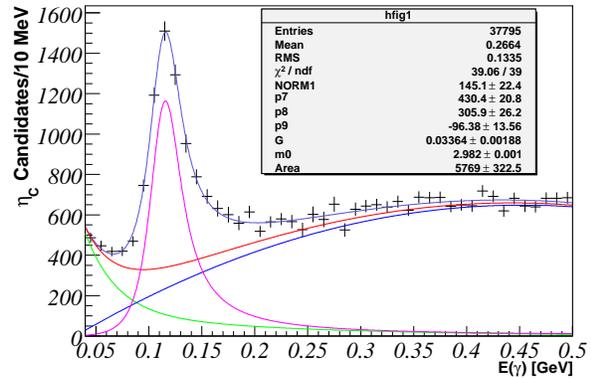
Fig. 1. Fit of CLEO data using $d\Gamma/d\omega \sim \omega^3\omega_0^2/(\omega\omega_0+(\omega-\omega_0)^2)BW(\omega)$.

In Table 1 results of fits with the CLEO function and our function are shown. We see that confidence levels are good in both cases.

Table 1.   Fit results of CLEO data using various decay probability functions.

$d\Gamma/d\omega$	$M(\eta_c), MeV/c^2$	$\Gamma(\eta_c), MeV$	N_{1S}^{EXC}	$\chi^2/NDF(C.L.)$
$\sim\omega^3 exp(-\omega^2/8\beta^2)BW(\omega)$	2982.4 ± 0.7	32.5 ± 1.8	6142 ± 430	$38.0/38$ (0.47)
$\sim\omega^3\omega_0^2/(\omega\omega_0+(\omega-\omega_0)^2)BW(\omega)$	2981.8 ± 0.5	33.6 ± 1.9	6494 ± 362	$39.1/39$ (0.47)

3 KEDR data

The experiment was performed at the KEDR detector[6] of the VEPP-4M collider[7]. In Fig. 2 a layout of the VEPP-4M collider is shown. It operates at a peak luminosity about $1.5 \cdot 10^{30}$ cm^{-2}s^{-1} near the J/ψ peak energy. Two methods of beam energy determination are used: resonant depolarization with accuracy of $8 \div 30$ keV and IR-light Compton backscattering with accuracy ~ 100 keV[8].

The view of the KEDR detector is shown in Fig. 3. Subsystems are listed in the figure. In this analysis a barrel liquid krypton calorimeter, drift chamber (DC) and time-of-flight (ToF) scintillator counters were of decisive importance. Luminosity was mea-

sured by single Bremsstrahlung online and by small angle Bhabha scattering offline.

This analysis is based on a data sample of 1.52 ± 0.08 pb^{-1} collected at the J/ψ peak. Three J/ψ scans were performed; a measured beam energy spread was used for the calculation of the number of J/ψ produced: $N_\psi = (5.9\pm0.3)\cdot 10^6$.

Event selection was done in two steps. At the first step multihadron decays of J/ψ were selected. To do this the following cuts were applied: total energy in clusters in calorimeters is greater than 0.8 GeV; at least 4 clusters with energy greater than 30 MeV in calorimeters are detected; at least one central track in the drift chamber is reconstructed; there are no muon tubes activated in the third layer. These cuts

effectively suppress background from the cosmic rays, beam-gas interactions and Bhabha events.
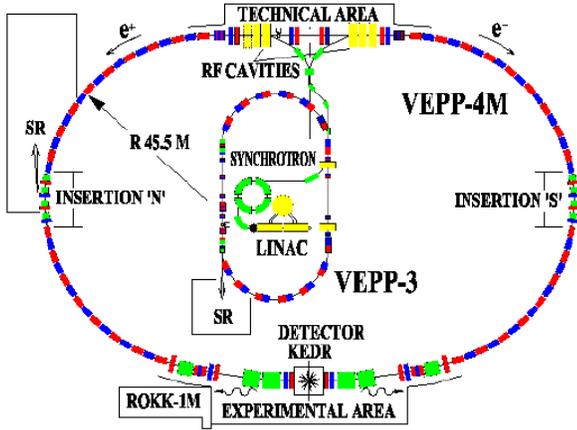
Fig. 2. VEPP-4M collider.
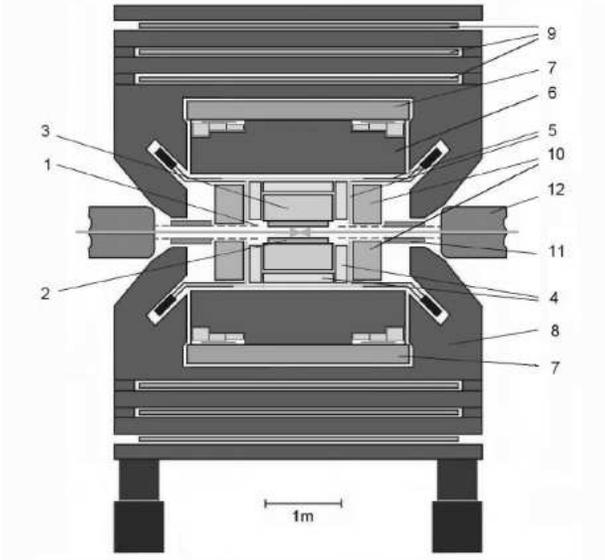
Fig. 3. KEDR detector. 1-vacuum chamber, 2-vertex detector, 3-drift chamber, 4-threshold aerogel counters, 5-ToF-counters, 6-liquid krypton calorimeter, 7-superconducting coil (0.65 T), 8-magnet yoke, 9-muon tubes, 10-CsI-calorimeter, 11-compensation solenoid, 12-VEPP-4M quadrupole.

At the second step photons in these events were identified. A photon is a cluster in the liquid krypton calorimeter without reconstructed tracks in the drift chamber attached to it and without ToF scintillator counters activated before the cluster. According to the simulation, the photon detection efficiency with the above mentioned cuts is about 34%.

4 Data analysis

The inclusive spectra of clusters are shown in Fig. 4. Large peaks in the spectra correspond to minimal ionizing particles crossing the calorimeter. The spectrum of charged particles was used to reject charged particles which were detected as neutrals from the photon spectrum during fitting procedure.
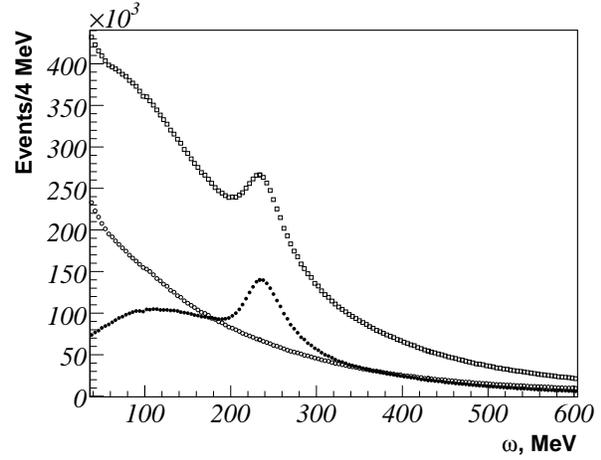
Fig. 4. Inclusive spectra in the liquid krypton calorimeter: open squares - all clusters; shaded circles - charged particles, when the ToF scintillator counter is activated before a cluster and a DC track is attached to cluster; open circles - photons.

In Fig. 5 a fit to our data is shown.
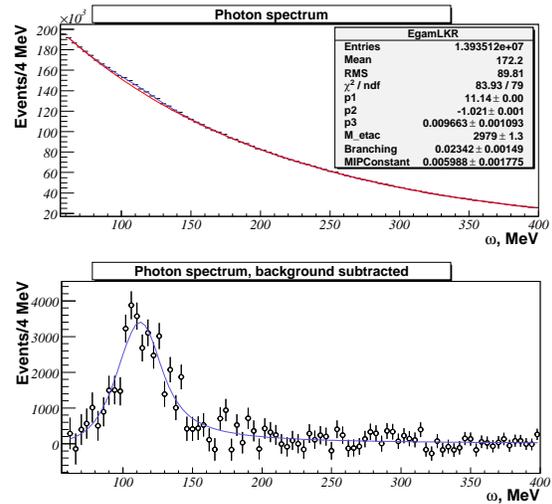
Fig. 5. Fit of the inclusive photon spectrum with $f(\omega) = \omega_0^2/(\omega\omega_0 + (\omega - \omega_0)^2)$.

The inclusive photon spectrum was fit by the sum of the signal having a shape $d\Gamma/d\omega \sim \omega^3 f(\omega) BW(\omega)$, convolved with the calorimeter response function (Novosibirsk PDF - asymmetric Gaussian with $\sigma_E = 8.8$ MeV at 110 MeV and a=-0.3), and background.
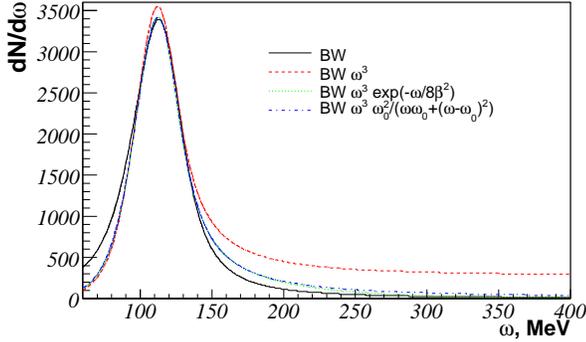
Fig. 6.   Resulting signal line shapes for various $d\Gamma/d\omega$ functions.

Background was taken in the form of exponent of a second-order polynomial plus a scaled histogram of charged particles. A relativistic Breit-Wigner function was used in the fit.

We also tried to fit our data with various line shapes. We used BW alone, $BW\cdot\omega^3$, CLEO function, and our function. The resulting signal line shapes for these functions are shown in Fig. 6. The BW function alone gives a shifted value of η_c mass compared to other functions: $M(\eta_c) = 2975.9 \pm 1.3$ MeV/c^2. $BW\cdot\omega^3$ gives a better form near the resonance, but leads to the unphysical diverging tail at higher photon energies. The last two functions give close results of fits, and their difference can be used for estimation of a systematic error appearing due to the unknown line shape. In Table 2 results of fits of KEDR data with the CLEO function and our function are listed. We see that confidence levels are good in both cases.

Table 2.   Fit results of KEDR data using various decay probability functions.

$d\Gamma/d\omega$	$M(\eta_c), MeV/c^2$	$\Gamma(\eta_c), MeV$	$\mathcal{B}(J/\psi \to \gamma\eta_c), \%$	$\chi^2/NDF(C.L.)$
$\sim \omega^3 exp(-\omega^2/8\beta^2)BW(\omega),\ \beta=65MeV$	2979.7 ± 1.6	26.9 ± 4.8	2.19 ± 0.28	$84.1/78\ (0.30)$
$\sim \omega^3\omega_0^2/(\omega\omega_0+(\omega-\omega_0)^2)BW(\omega)$	2979.4 ± 1.5	27.8 ± 5.1	2.36 ± 0.34	$83.9/78\ (0.30)$

5   Systematic errors

In Table 3 systematic errors of our measurements are listed. Systematic error appearing due to the unknown line shape was estimated using various line shapes and fixing η_c width to the current PDG values (27.4 ± 2.9 MeV). Systematic error related to the background subtraction was estimated by the taking a polynomial of the third order instead of the second in the fit, and varying ranges of the fit. Luminosity measurement error was evaluated from the difference between the measured and calculated number of the multihadron J/ψ decays. Photon detection efficiency is conservatively estimated as 10%. Photon energy scale calibration was made comparing a π^0 peak position in simulation and data.

Table 3.   Systematic errors.

Systematic error	$M(\eta_c), MeV/c^2$	$\Gamma(\eta_c), MeV$	$\mathcal{B}(J/\psi \to \gamma\eta_c), \%$
Line shape	1.5	2.5	0.25
Background subtraction	0.5	2.2	0.18
Luminosity measurement			0.11
Photon efficiency			0.23
Photon energy scale	1.1		
Total	1.9	3.3	0.40

6   Results and conclusions

A new direct measurement of $J/\psi \to \eta_c\gamma$ decay was performed. We measured η_c mass, width, and branching fraction of $J/\psi \to \eta_c\gamma$ decay. Our preliminary results are:

$M(\eta_c) = 2979.4\pm1.5\pm1.9$ MeV/c^2,
$\Gamma(\eta_c) = 27.8\pm5.1\pm3.3$ MeV,
$\mathcal{B}(J/\psi \to \eta_c\gamma) = (2.34\pm0.15\pm0.40)\%$.

In Fig. 7 results of our measurements, compared with the other experiments and the current PDG values, are shown. The branching fraction of this decay is sensitive to the line shape, which is asymmetric, and it should be taken into account during a measurement.

We see that our results on η_c mass and width are consistent with the current PDG values. Our result for $\mathcal{B}(J/\psi \to \eta_c\gamma)$ is consistent with that of CLEO, is higher than the old Crystal Ball value and close to theoretical predictions.
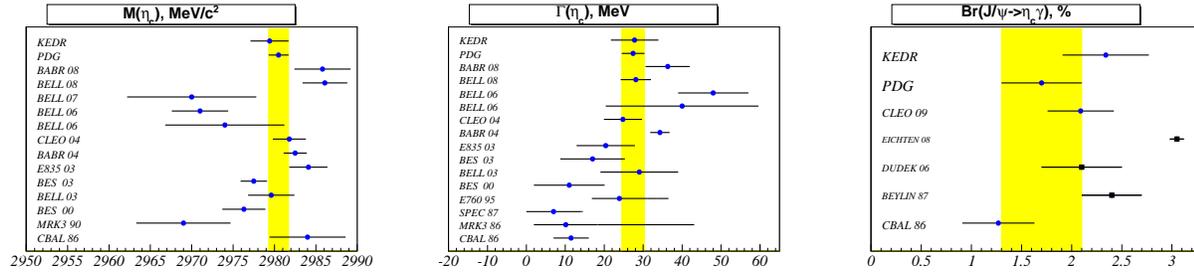
Fig. 7. η_c mass, width and $\mathcal{B}(J/\psi \to \eta_c\gamma)$ measurements. The theoretical predictions for the branching fraction are also shown (squares).

References

1 J.Gaiser et al., Phys. Rev. D, 1986, **34**: 711

2 E.E. Eichten et al., Rev.Mod.Phys., 2008, **80**: 1161-1193

3 V.A. Beilin, A.V. Radyushkin, Sov.J.Nucl.Phys., 1987, **45**: 342

4 J.J. Dudek et al., Phys. Rev. D, 2006, **73**: 07450

5 R.E. Mitchell et al., Phys. Rev. Lett., 2009, **102**: 011801

6 V.V. Anashin et al., Nuclear Instruments and Methods, 2002, **A478**: 420.

7 V. Anashin et al., Stockholm 1998, EPAC 98*, 400 (1998), Prepared for 6th European Particle Accelerator Conference (EPAC 98), Stockholm, Sweden, 22-26 Jun 1998.

8 V.E. Blinov et al., Nucl. Instr. and Meth., 2009, **A598**: 23